

web page: <http://w3.pppl.gov/~zakharov>

# Consideration of variances in equilibrium reconstruction<sup>1</sup>

**Leonid Zakharov**

*Princeton Plasma Physics Laboratory, MS-27*

*P.O. Box 451, Princeton NJ 08543-0451*

*in collaboration with*

***Jill E.L. Foley, Fred M. Levinton, and Howard Y. Yuh***

*Nova Photonics*

*Science meeting,*

*April 20, 2007, GA San Diego CA*

## Abstract

---

*The talk presents a theory of uncertainties in the reconstructions of the plasma current density and pressure profiles in the Grad-Shafranov equation. The associated technique was incorporated into the ESC code.*

*Potential variances in  $q$ - and  $p$ - profiles have been calculated for different sets of external and internal measurements envisioned for equilibrium reconstruction in ITER.*

*It was shown that complementing the external magnetic measurements with either Stark line polarization signals (MSE-LP) or with recently proposed for ITER by Nova Photonics line shift signals (MSE-LS) can significantly improve the reliability of the reconstructed plasma profiles and the magnetic configuration.*

*Capabilities of calculating variances, incorporated into the numerical code ESC, have completed the theory of reconstruction, which for a long time had a significant gap in ability to evaluate the quality of the presently widely used equilibrium reconstruction technique.*

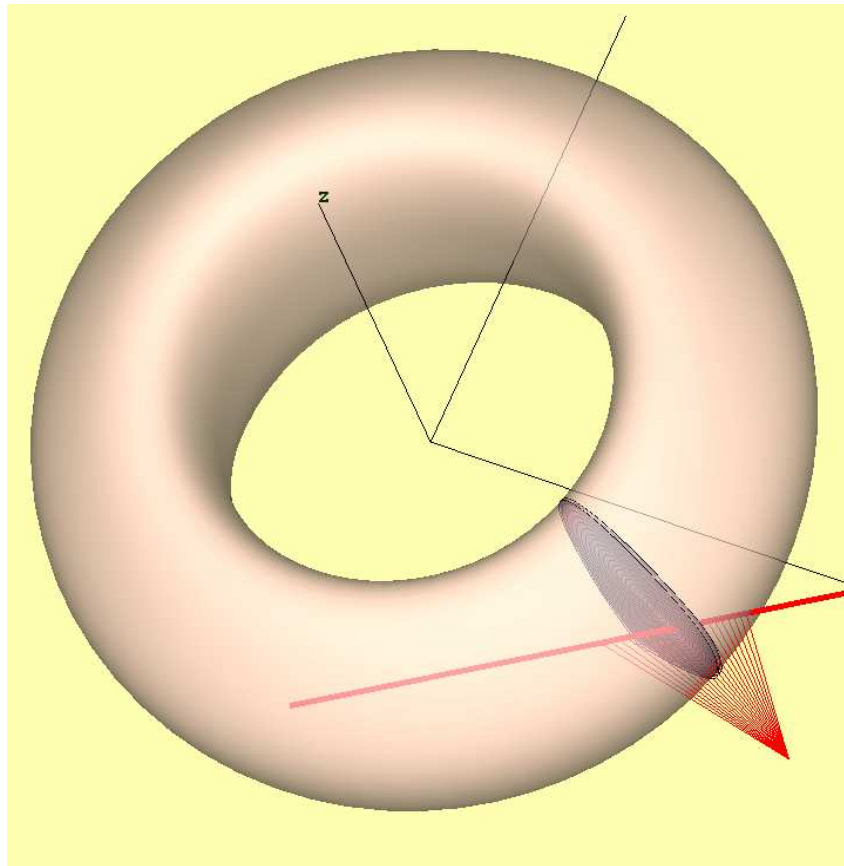
# Contents

---

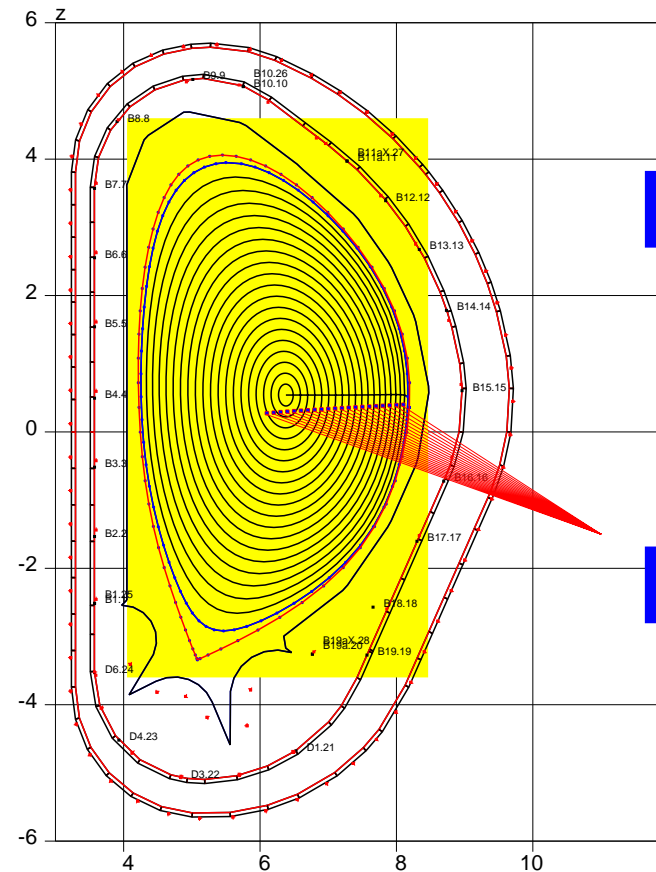
1	Set of signals for equilibrium reconstruction	4
2	Variances in tokamak equilibrium reconstruction	6
3	“Rigorous” theory for “non-rigorous” reality	9
4	Capabilities of diagnostics for equilibrium reconstruction	12
4.1	<i>Good looking magnetic only reconstruction . . . . .</i>	14
4.2	<i>Magnetic signals &amp; MSE-LP . . . . .</i>	18
4.3	<i>Magnetic signals &amp; line shift MSE-LS . . . . .</i>	21
4.4	<i>Magnetic signals &amp; both MSE-LP &amp; MSE-LS . . . . .</i>	26
4.5	<i>Free boundary, magnetic signals &amp; both MSE-LP &amp; MSE-LS . . . . .</i>	28
4.6	<i>Curious case, NO B-signals, <math>\xi \neq 0</math>, <math>\Phi</math> &amp; both MSE-LP &amp; MSE-LS . . . . .</i>	30
5	Summary	32

# 1 Set of signals for equilibrium reconstruction

**ITER  $B=5.3$  T,  $I_{pl}=15$  MA  $\beta = 2.8\%$  equilibrium configuration**



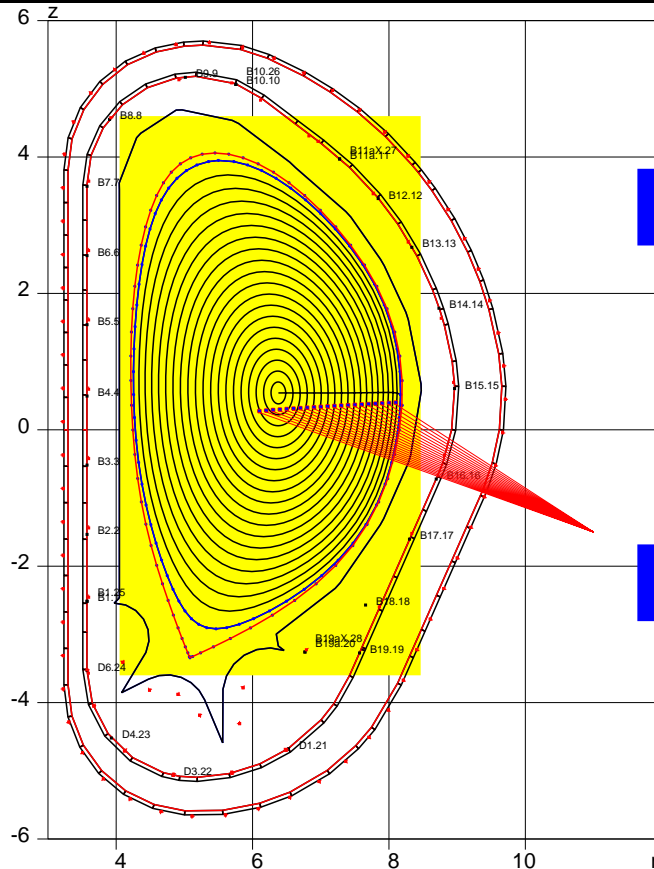
Center line of 1 MeV NBI in ITER



$\Psi$ -loops, B-coils, pickup points of MSE

**One of unique features of ITER is its 1 MeV neutral beam injection**

# Measurements of the Line Shift due to MSE was proposed by Nova Photonics as a diagnostics of ITER configuration



Reference signal errors  $\epsilon$  used here for calculating variances in equilibrium reconstruction in ITER:

Signal name	$\epsilon^{relative}$	$\epsilon^{absolute}$	Comment
B-coils	0.01	0.01 T	<i>local probes</i>
$\Psi$ -loops	0.01	0.001 Vsec	
$\Phi$ -loop	0.01	0.001 Vsec	<i>diamagnetic loop</i>
MSE-LP	0.01	$0.1^\circ$	$B_z/B_\phi$ from MSE <i>line polarization</i>
MSE-LS	0.01	0.05 T	$\sqrt{ B ^2 - (B \cdot v)^2}$ <i>from MSE line shift</i>

MSE-LP and MSE-LS signals were assumed to be point-wise. This requires more realistic model from Nova Photonics.

**The capabilities of equilibrium reconstruction with such a set of signal is the topic of the talk**

## 2 Variances in tokamak equilibrium reconstruction

**The practice typically neglects making analysis of variances in reconstructed equilibria**

*In tokamaks the Grad-Shafranov (GSh) equation describes the configuration*

$$\Delta^* \bar{\Psi} = -T(\bar{\Psi}) - P(\bar{\Psi})r^2, \quad T \equiv \bar{F} \frac{d\bar{F}}{d\bar{\Psi}}, \quad P \equiv \mu_0 \frac{dp}{d\bar{\Psi}}, \quad (2.1)$$

*Its solution can be perturbed by*

*1. perturbation of the plasma shape*

$$\xi(a_{pl}, l), \quad \text{and} \quad (2.2)$$

*2. perturbation of two 1-D functions*

$$\delta T(\bar{\Psi}), \quad \delta P(\bar{\Psi}). \quad (2.3)$$

*The question, neglected by present practice, is what level of perturbations cannot be distinguished given the finite accuracy of measurements.*

**The level of variances  $\xi$ ,  $\delta T$ ,  $\delta P$  determines the very value of reconstruction and of the entire diagnostics system**

**The theory of variances has been created in 2006 by L.Zakharov, J.Levandowski, V.Drozdo and D.McDonald**

*The problem is reduced to solving the linearized equilibrium problem*

$$\bar{\Psi} = \bar{\Psi}_0 + \psi, \quad \Delta^* \psi + T'_{\bar{\Psi}} \psi + P'_{\bar{\Psi}} \psi = -\delta T(a) - \delta P(a)r^2 \quad (2.4)$$

*for  $N$  possible perturbations*

$$\xi = \sum_{n=0}^{n < N_{\xi}} A_n \xi^n(l), \quad \delta T = \sum_{n=0}^{n < N_J} T_n f^n, \quad \delta P = \sum_{n=0}^{n < N_P} P_n f^n, \quad (2.5)$$

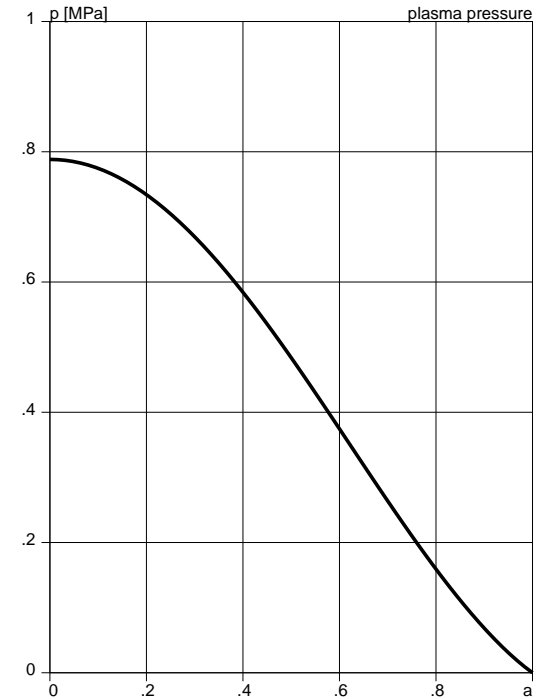
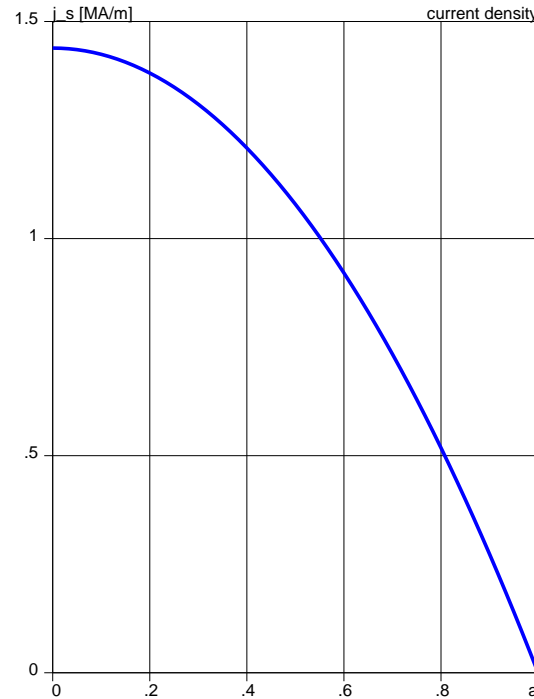
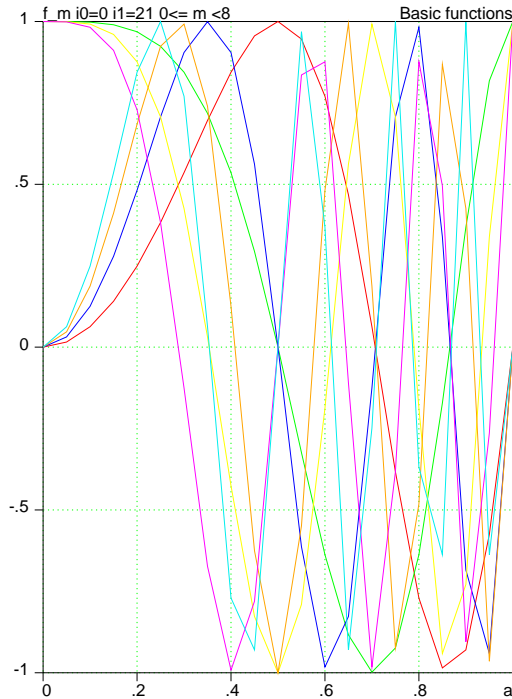
$$N = N_{\xi} + N_J + N_P, \quad f^{2n} = \cos 2\pi n a^2, \quad f^{2n+1} = \sin 2\pi n a^2,$$

*where  $l$  is the poloidal coordinate at the plasma boundary, and  $0 \leq a \leq 1$  is the square root from the normalized toroidal flux.*

*The response of the diagnostics to each of  $N$  solutions  $\psi^n$  can be calculated in a straightforward way.*

**ESC is based on linearization of the GSh equation. It was complemented with a routine for analysis of variances**

8 functions  $f^n(a^2)$  has been used to perturb  $P(\bar{\Psi}), T(\bar{\Psi})$



Trigonometric expansion functions  $f^n(a^2)$       background current density profiles  $\bar{j}_s(a)$       background pressure profile  $\bar{p}(a)$

**ESC can use an extended set of basis functions**



### 3 “Rigorous” theory for “non-rigorous” reality

**After solving the perturbed GSh equation, the problem is reduced to a matrix problem**

Let vector  $\vec{X}$  contains the amplitudes of perturbations

$$\vec{X} \equiv \left\{ \underbrace{A_0, A_1, \dots, A_{N_b-1}}_{N_\xi \text{ of } \xi}, \underbrace{T_0, \dots, T_{N_T-1}}_{N_T \text{ of } \delta T}, \underbrace{P_0, \dots, P_{N_P-1}}_{N_P \text{ of } \delta P} \right\} \quad (3.1)$$

and vector  $\delta\vec{S}$  represents the signals

$$\delta\vec{S} \equiv \left\{ \underbrace{\delta\Psi_0, \dots, \delta\Psi_{M_\Psi-1}}_{M_\Psi \text{ of } \delta\Psi}, \underbrace{\delta B_0, \dots, \delta B_{M_B-1}}_{M_B \text{ of } \delta B_{pol}}, \underbrace{\delta S_0, \dots, \delta S_{M_S-1}}_{M_S \text{ of } \delta\text{others}} \right\}, \quad (3.2)$$

$$M \equiv M_\Psi + M_B + M_S, \quad M > N.$$

32  $\Psi$ -, 1  $\Phi_{diamagnetic}$ -loops, 64  $B$ -probes, 21 MSE-LP (line polarization) and 21 MSE-LS (line shift) signals (both pointwise) were used in the analysis.

**ESC calculates the response matrix  $A$  relating  $\delta\vec{S}$  and perturbations  $\delta\vec{X}$**

$$\delta\vec{S} = A\vec{X}, \quad A = A_{M \times N}. \quad (3.3)$$

## The working matrix $\bar{A}$ weights $\delta S_m$ based on their accuracy

$$(\bar{A})_m^n = \frac{1}{\epsilon_m} (A)_m^n, \quad \delta \bar{S}_m = \frac{1}{\epsilon_m} \delta S_m, \quad \bar{A} \vec{X} = \delta \vec{S}, \quad (3.4)$$

where  $\epsilon_m$  is the error in the signal  $S_m$ . SVD expresses the matrix  $\bar{A}$  as a product

$$\begin{aligned} \bar{A} &= U \cdot W \cdot V^T, \\ U &= U_{M \times N}, \quad U^T \cdot U = I, \quad I_m^n = \delta_m^n, \\ W &= W_{N \times N}, \quad W_k^n = w^n \delta_k^n, \\ V &= V_{N \times N}, \quad V^T \cdot V = I. \end{aligned} \quad (3.5)$$

Here,  $w^n$  are the eigenvalues of the matrix problem.

The resulting vector of variances can be represented as a linear combination of “eigenvectors”, which are the columns of matrix  $V$

$$\vec{X}^k = \vec{V}^k, \quad A \vec{X}^k = w^k \vec{U}^k, \quad \bar{\sigma}^k \equiv \sqrt{\frac{1}{M} \sum_{m=0}^{m \leq M} (A \vec{X}^k)_m^2} = \frac{w^k}{\sqrt{M}}, \quad (3.6)$$

Eq.(3.6) gives variances and normalized RMS  $\bar{\sigma}^k$  in an explicit form. The

perturbations  $\vec{X}^k$  with  $\bar{\sigma}^k > 1$  are “invisible” for diagnostics

## SVD of matrix A

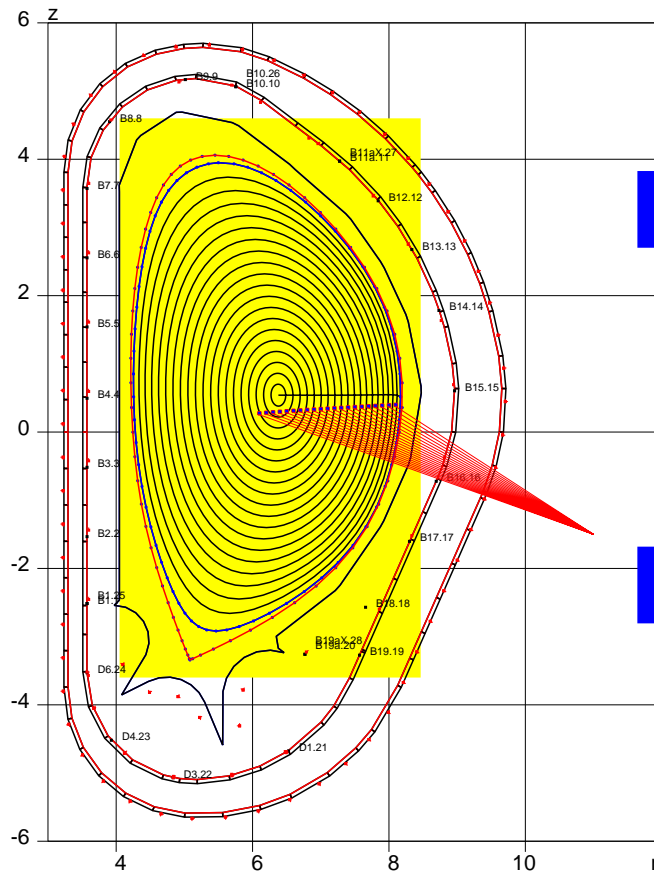
$$\begin{pmatrix} \dots & \dots \\ & A \\ \dots & \dots \\ (M) & \end{pmatrix} \begin{pmatrix} (N) \\ \dots & \dots \\ & U \\ \dots & \dots \\ (M) & \end{pmatrix} = \begin{pmatrix} w_1 & \dots & \dots \\ \dots & w_k & \dots \\ \dots & \dots & w_N \end{pmatrix} \times \begin{pmatrix} \dots & (N) \\ & \dots \\ V & \\ \dots & \dots \\ (N) & \end{pmatrix} \quad (3.7)$$

Vector  $\vec{X}$  in terms of eigen-vectors

$$\begin{pmatrix} X_1 \\ \dots \\ \vec{X} \\ \dots \\ X_N \end{pmatrix} = \begin{pmatrix} \dots & (N) \\ & \dots \\ V & \\ \dots & \dots \\ (N) & \end{pmatrix} \times \begin{pmatrix} C_1 \\ \dots \\ \vec{C} \\ \dots \\ C_N \end{pmatrix} \quad (3.8)$$

## 4 Capabilities of diagnostics for equilibrium reconstruction

### ITER configuration is used for illustrating the technique



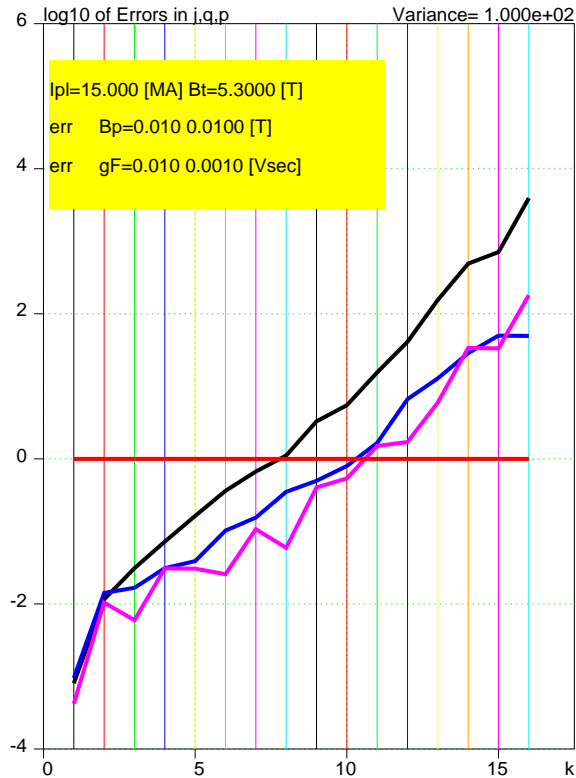
Reference signal errors  $\epsilon$  used here for calculating variances in equilibrium reconstruction in ITER:

Signal name	$\epsilon^{relative}$	$\epsilon^{absolute}$	Comment
B-coils	0.01	0.01 T	<i>local probes</i>
$\Psi$ -loops	0.01	0.001 Vsec	
$\Phi$ -loop	0.01	0.001 Vsec	<i>diamagnetic loop</i>
MSE-LP	0.01	$0.1^\circ$	<i><math>B_z/B_\phi</math> from MSE line polarization</i>
MSE-LS	0.01	0.05 T	<i><math>\sqrt{ B ^2 - (B \cdot v)^2}</math> from MSE line shift</i>

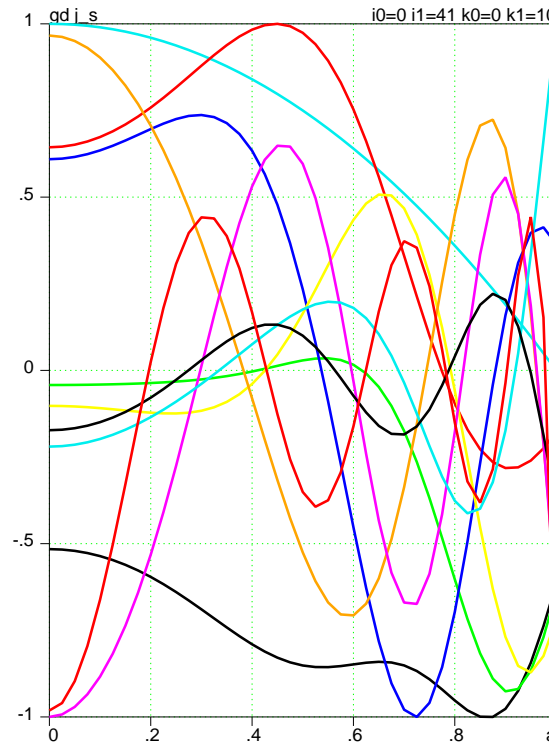
MSE-LP and MSE-LS signals were assumed to be point-wise. This requires more realistic model from Nova Photonics.

**Different combinations of signal lead to different residual variances**

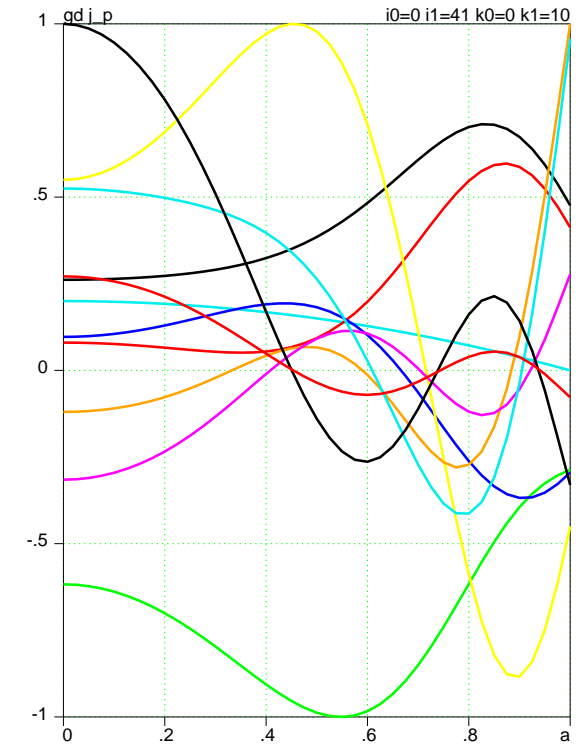
**Plasma boundary is well specified,  $\Phi$ -loop,  $B$ -coils are used**



$\log_{10} \bar{\sigma}^k$ ,  $\log_{10} \bar{\sigma}_q^k$ ,  $\log_{10} \bar{\sigma}_p^k$   
 ( $N_J = 8$ ,  $N_P = 8$ )



Eigen-variances  $\delta j_s^k(a)$ .

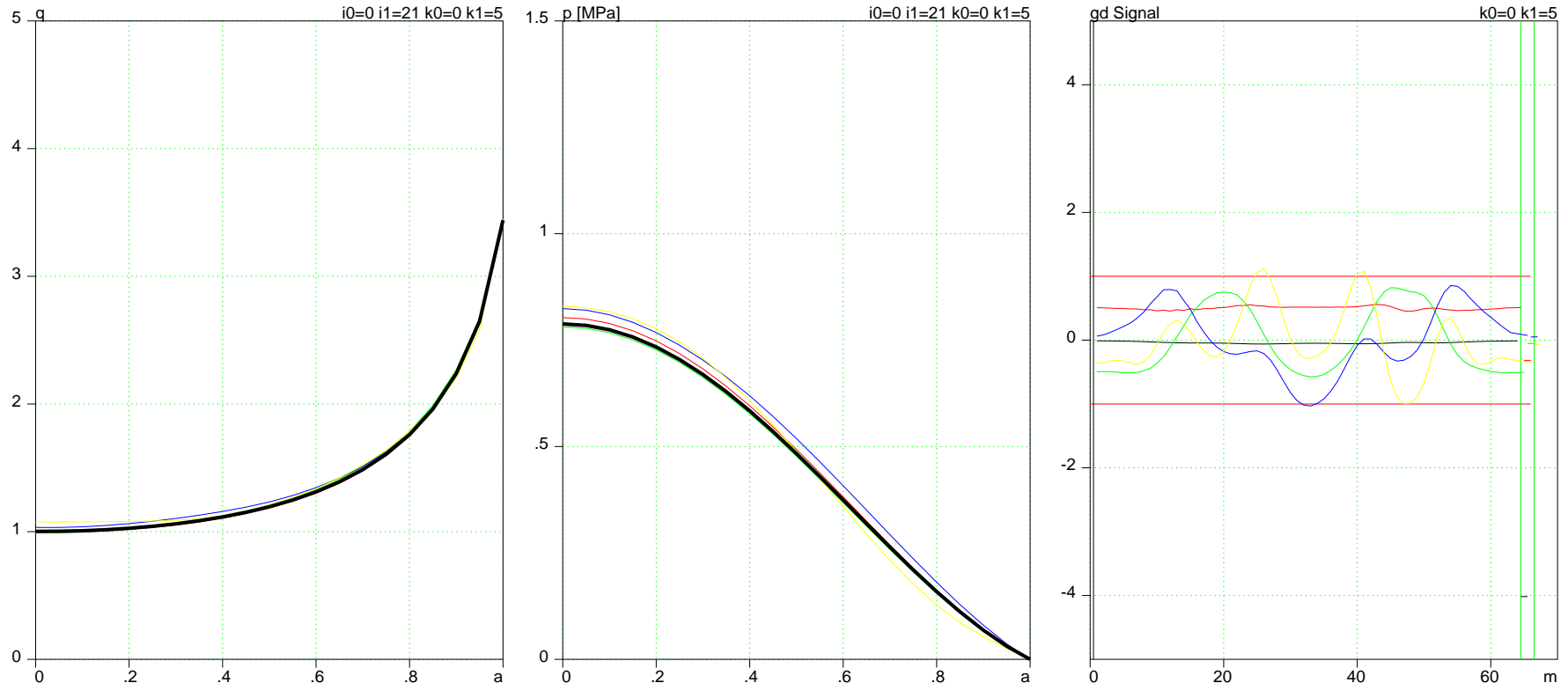


Eigen-variances  $\delta j_p^k(a)$ ,  
 $j_p \equiv P/R_0$

$\bar{\sigma}_q$  and  $\bar{\sigma}_p^k$  [MPa] on the left plot are RMS for  $q$ - and  $p$ -profiles

**Perturbations  $j_s^k > 8$ ,  $j_p^k > 8$  are invisible and cannot be reconstructed**

**Plasma boundary is well specified,  $\Phi$ -loop,  $B$ -coils are used**



$q$ — profile and variances for  $k_J \leq 3, k_P \leq 2$

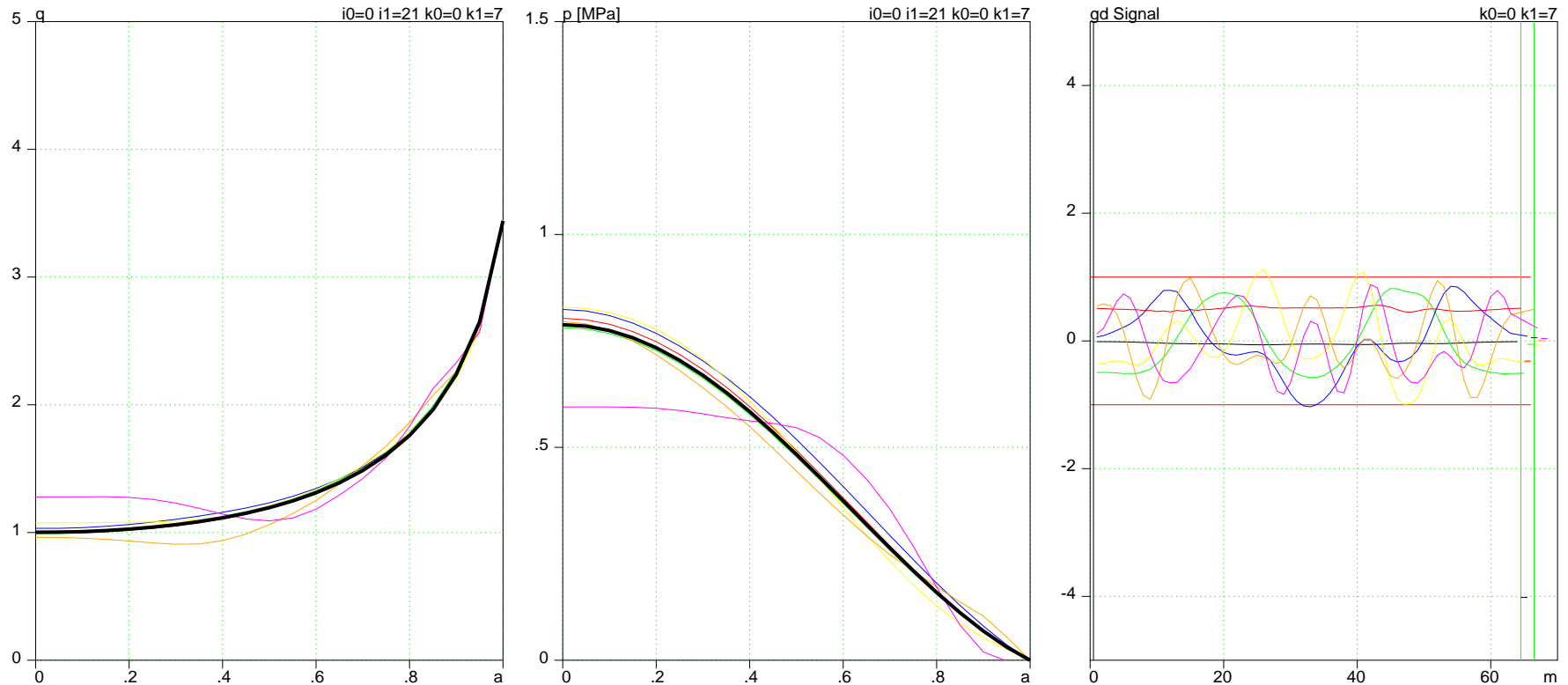
variances in  $p$ —profile as functions of  $a$

Signals  $\delta S_m / \epsilon_m$  generated by perturbations

**For  $k_J + k_P = 5$ , typically used, the reconstruction looks very good**

**KiloGb's of reconstructions "data" can be easily generated**

**Plasma boundary is well specified,  $\Phi$ -loop,  $B$ -coils are used**



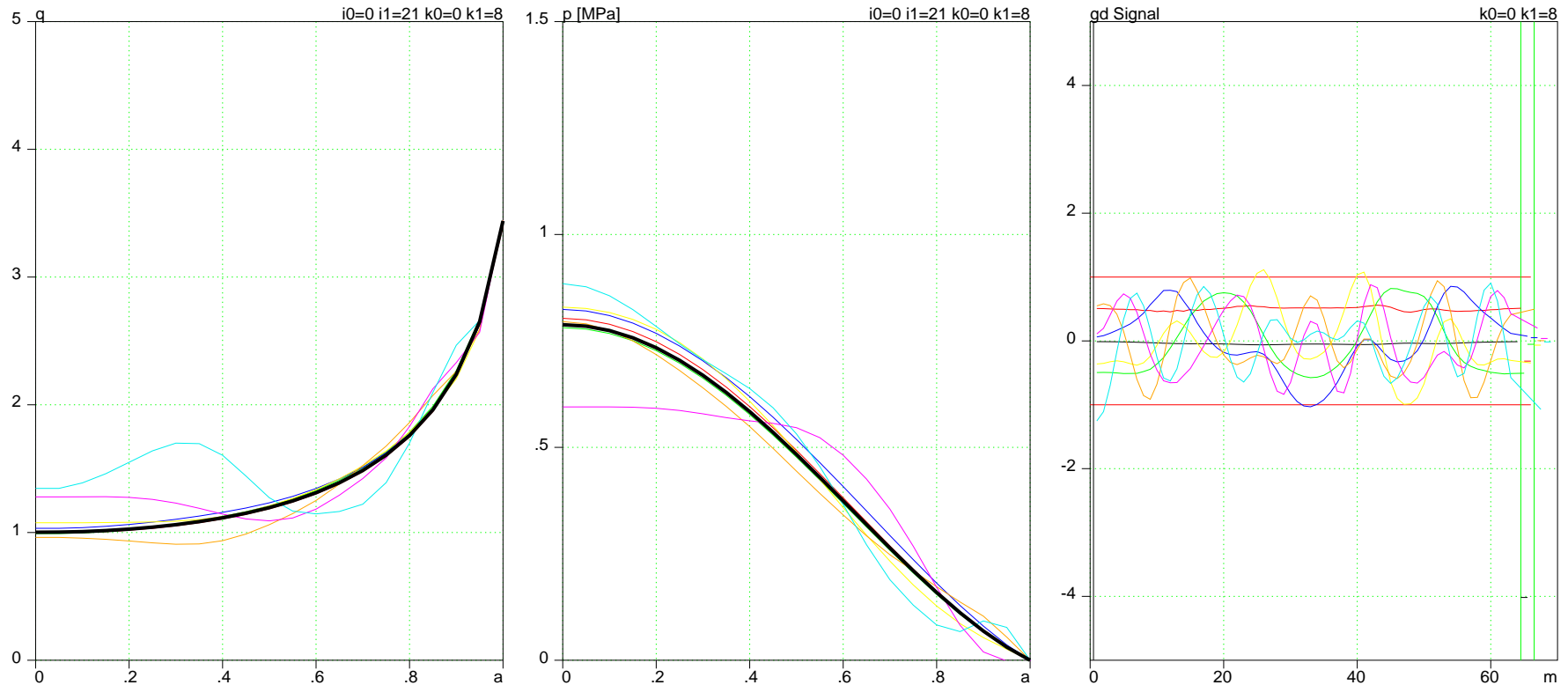
$q$ — profile and variances for  $k_J \leq 4, k_P \leq 3$ .

$p$ — profile and its variances as functions of  $a$

Signals  $\delta S_m / \epsilon_m$  generated by perturbations

**Testing  $k_J+k_P=7$  shows that the reconstruction is, in fact, not so good**

**Plasma boundary is well specified,  $\Phi$ -loop,  $B$ -coils are used**



$q$ — profile and variances for  $k_J \leq 4, k_P \leq 4$

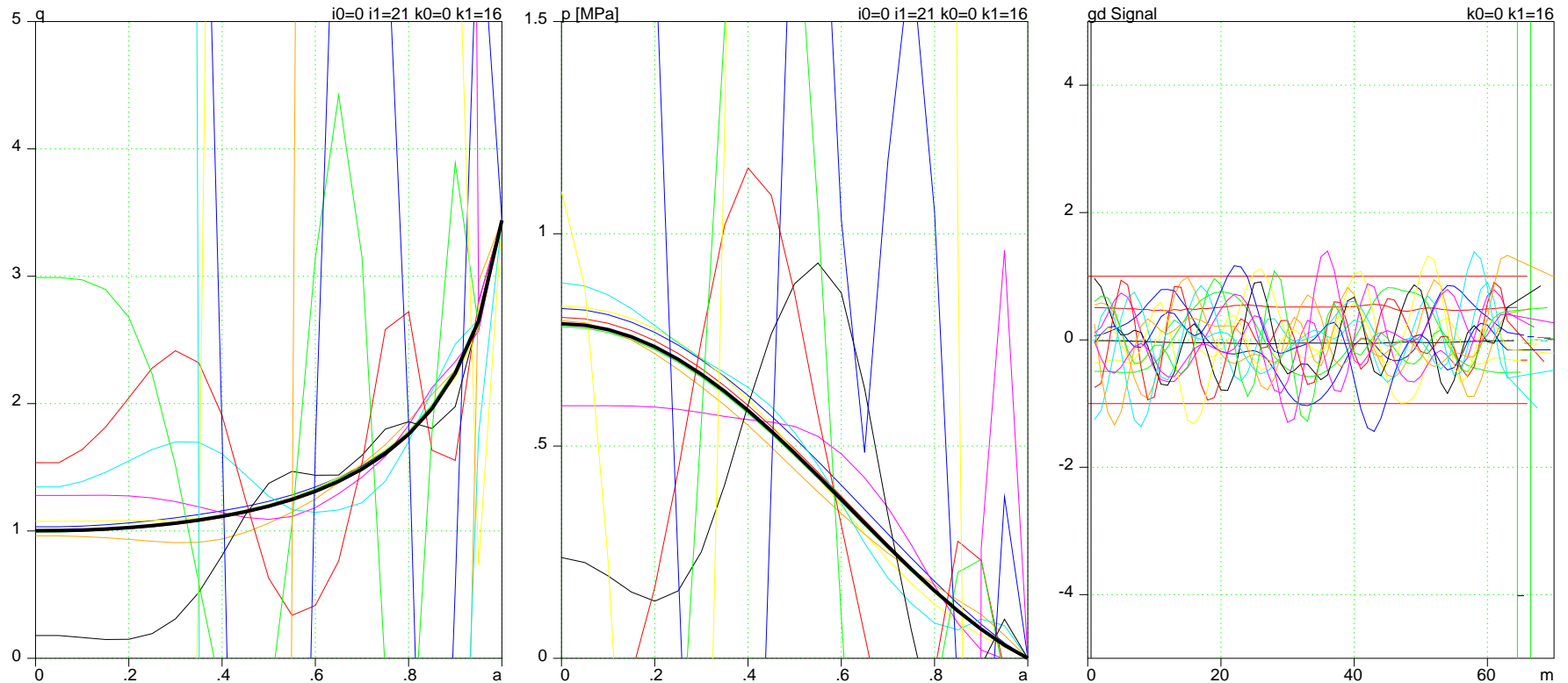
$p$ — profile and its variances as functions of  $a$

Signals  $\delta S_m / \epsilon_m$  generated by perturbations

**Testing  $k_J+k_P=8$  shows that even the  $q$  reconstruction is doubtful**



**Plasma boundary is well specified,  $\Phi$ -loop,  $B$ -coils are used**



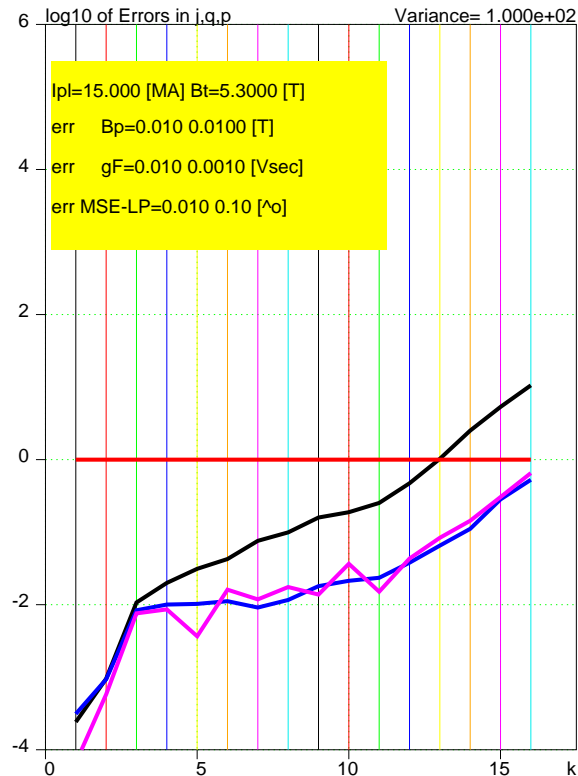
$q$ — profile and variances for  $k_J \leq 8, k_P \leq 8$

$p$ — profile and its variances as functions of  $a$

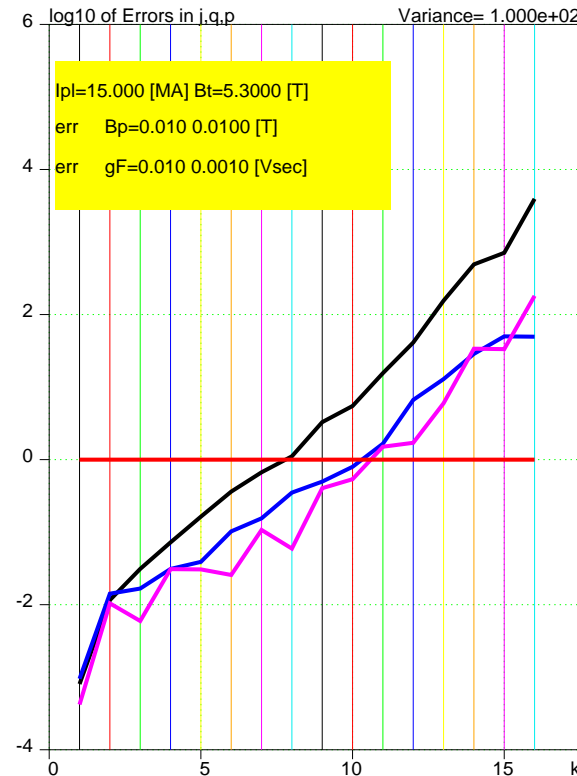
Signals  $\delta S_m / \epsilon_m$  generated by perturbations

**Test of  $k_J + k_P = 16$  shows that with no constraints the reconstruction has no scientific value and is a sort of “beliefs”**

# Fixed plasma boundary with ( $\Phi$ & $B$ & MSE-LP) signals



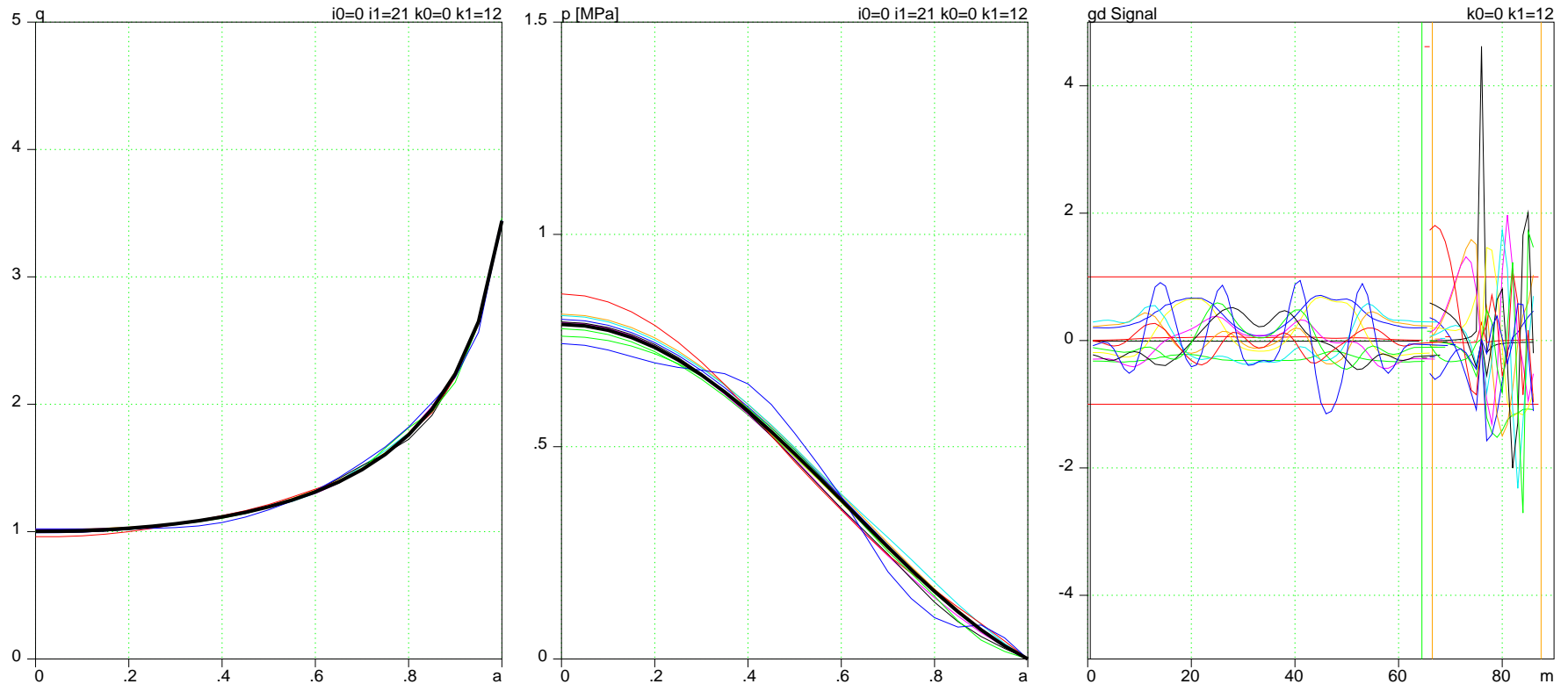
$\log_{10} \bar{\sigma}^k$ ,  $\log_{10} \bar{\sigma}_q^k$ ,  $\log_{10} \bar{\sigma}_p^k$   
in case of  $\Phi$  &  $B$  & MSE-LP



$\log_{10} \bar{\sigma}^k$ ,  $\log_{10} \bar{\sigma}_q^k$ ,  $\log_{10} \bar{\sigma}_p^k$   
in case of  $\Phi$  &  $B$  only

**Use of MSE-LP drops largest RMS  $\bar{\sigma}$ , makes 12 perturbations visible, and dramatically improves reconstruction of  $q, p$**

**Fixed plasma boundary with ( $\Phi$  &  $B$  & MSE-LP) signals**



$q$ — profile and variances for  $k_J \leq 6, k_P \leq 6$

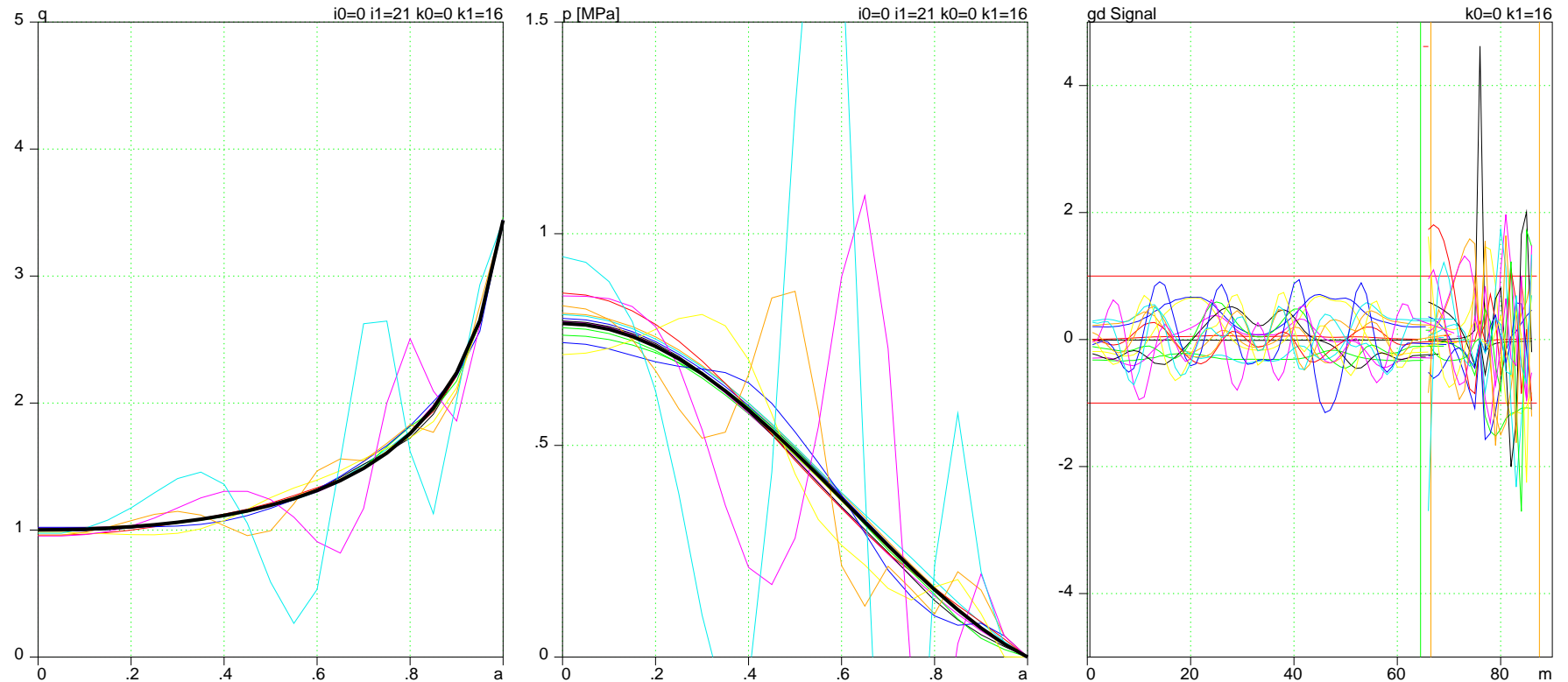
$p$ — profile and its variances as functions of  $a$

Signals  $\delta S_m / \epsilon_m$  generated by perturbations

**Testing  $N = 12$  shows that MSE-LP allows to reconstruct both**

**q- and p-profiles**

## Fixed plasma boundary with ( $\Phi$ & $B$ & MSE-LP) signals



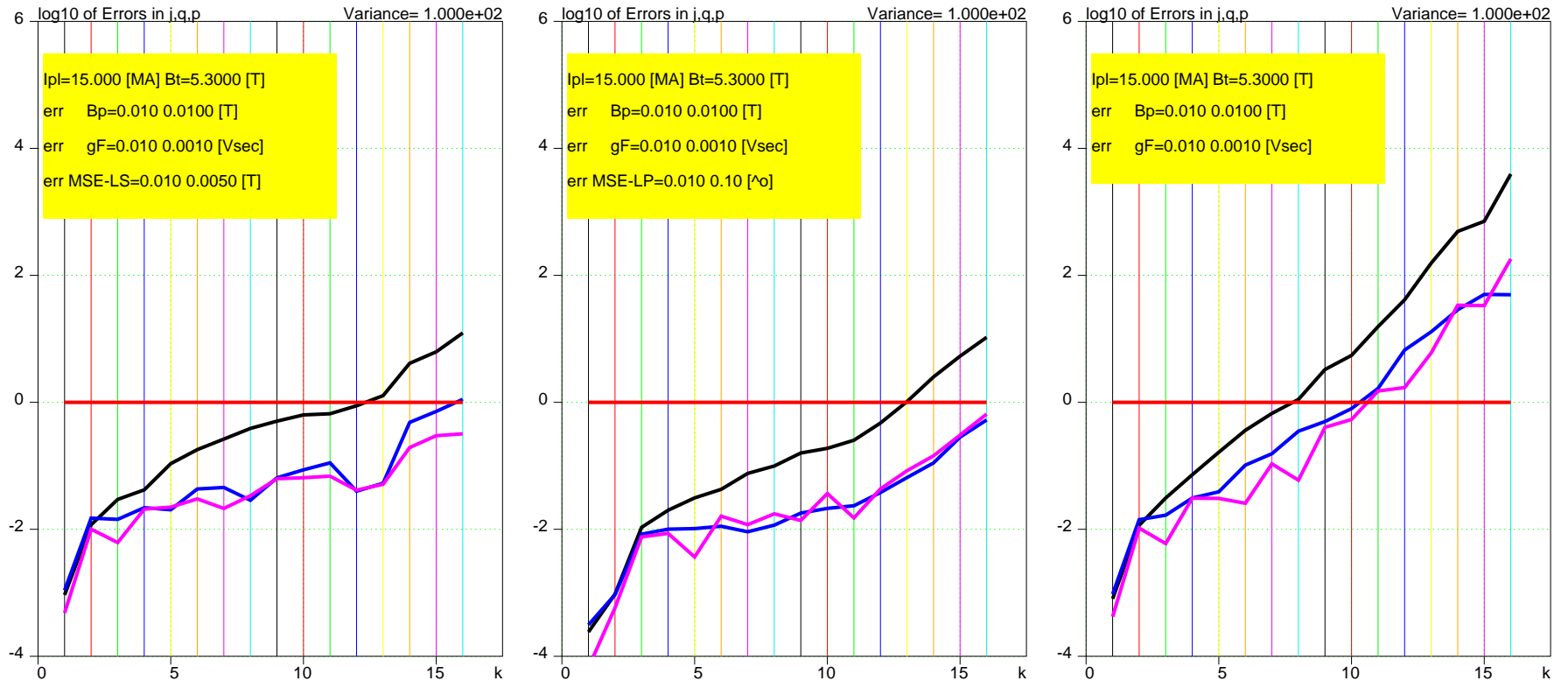
$q$ — profile and variances for all  $k$

$p$ — profile and its variances as functions of  $a$

Signals  $\delta S_m / \epsilon_m$  generated by perturbations

**Only perturbations with  $k \geq 14$  might be potentially troublesome**

## Fixed plasma boundary with ( $\Phi$ & $B$ & MSE-LS) signals



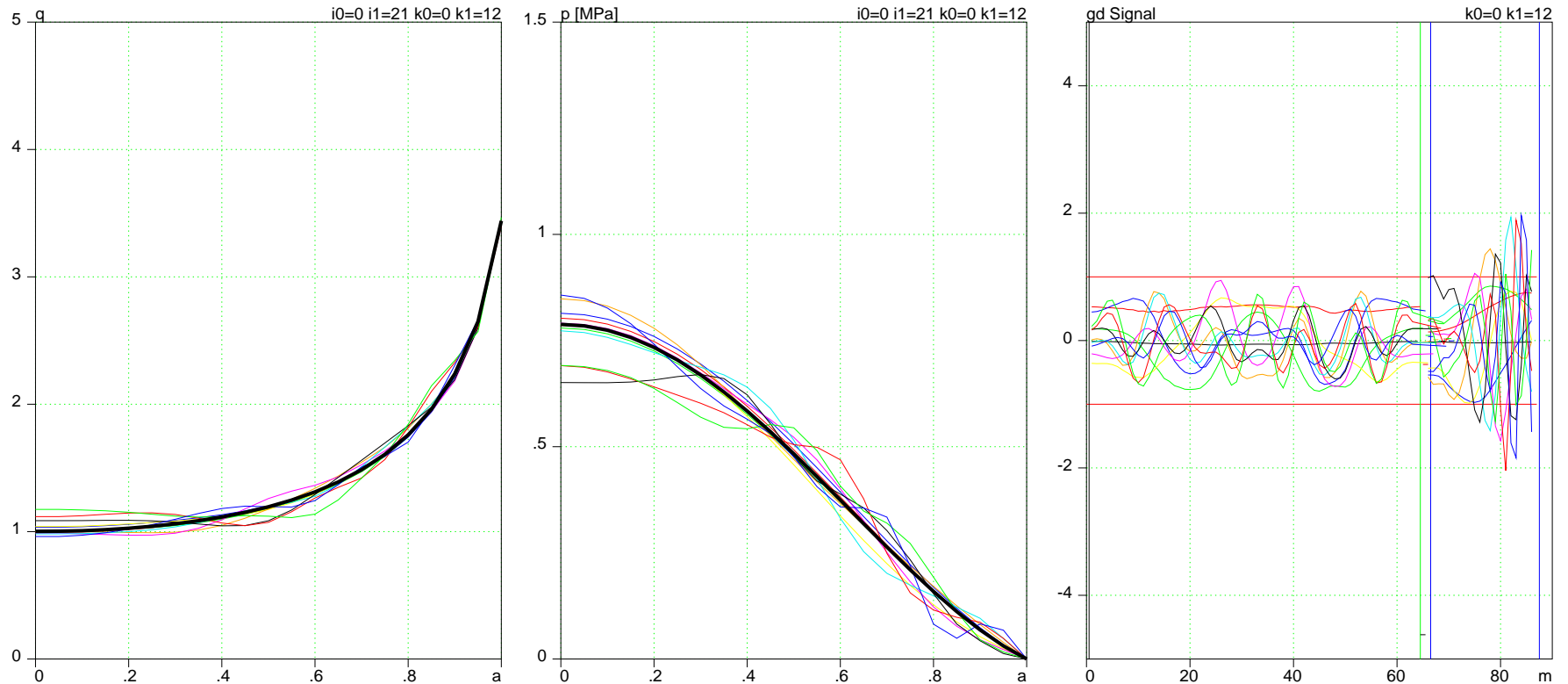
$\log_{10}\{\bar{\sigma}^k, \bar{\sigma}_q^k, \bar{\sigma}_p^k\}$  in case of ( $\Phi$  &  $B$  & MSE-LS)

$\log_{10}\{\bar{\sigma}^k, \bar{\sigma}_q^k, \bar{\sigma}_p^k\}$  in case of ( $\Phi$  &  $B$  & MSE-LP)

$\log_{10}\{\bar{\sigma}^k, \bar{\sigma}_q^k, \bar{\sigma}_p^k\}$  in case of ( $\Phi$  &  $B$ ) only

**Use of MSE-LS can compete with MSE-LP in its value for reconstruction**

## Fixed plasma boundary with ( $\Phi$ & $B$ & MSE-LS) signals



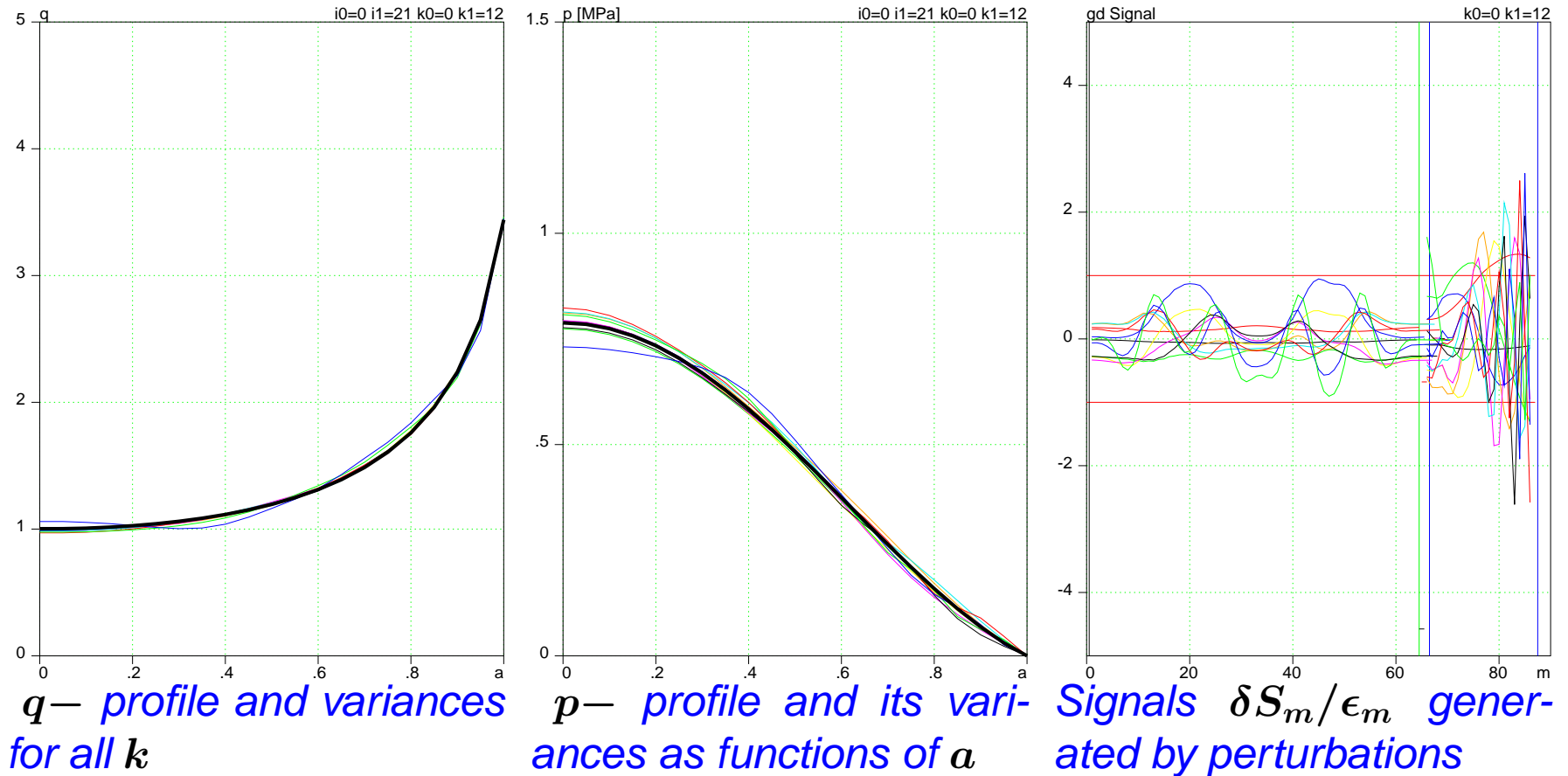
$q$ — profile and variances for all  $k$

$p$ — profile and its variances as functions of  $a$

Signals  $\delta S_m / \epsilon_m$  generated by perturbations

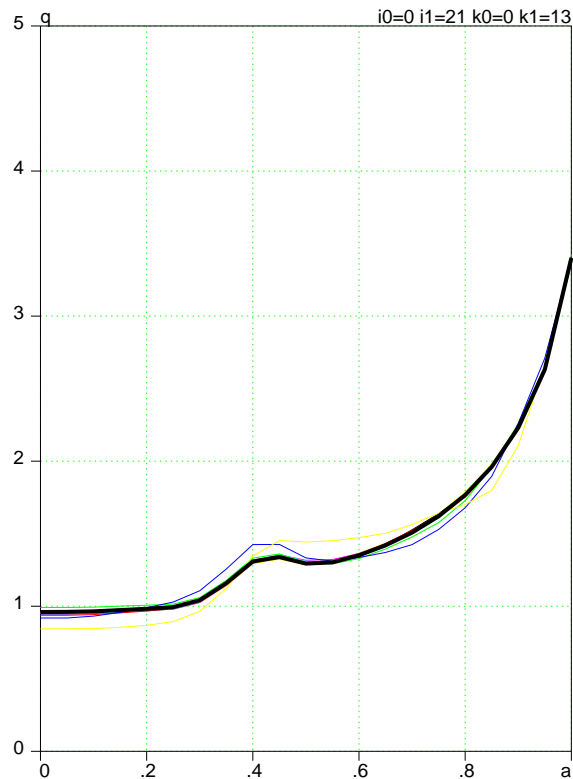
**Perturbations with  $k \leq 12$  can be reconstructed using MSE-LS**

Same case with the improved relative accuracy of MSE-LS

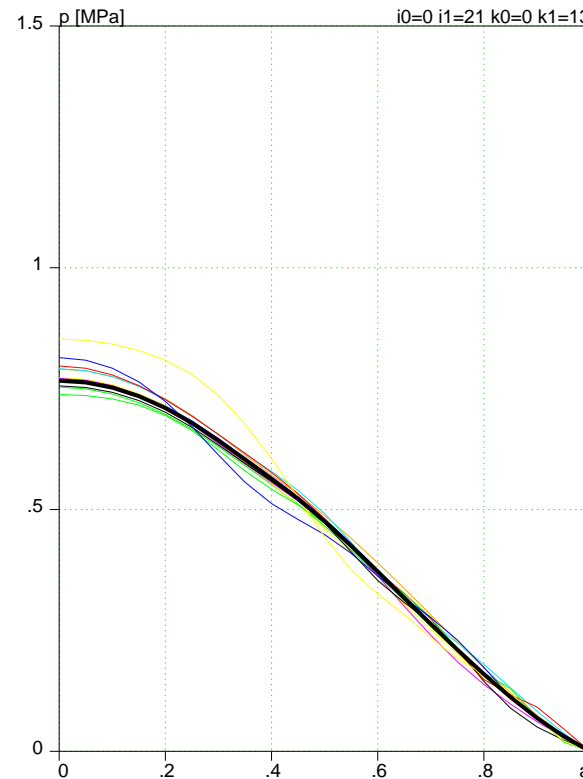


A realistic reduction of relative error  $\epsilon_{MSE-LS}^{relative} \rightarrow 0.1\%$  improves the pressure profile reconstruction

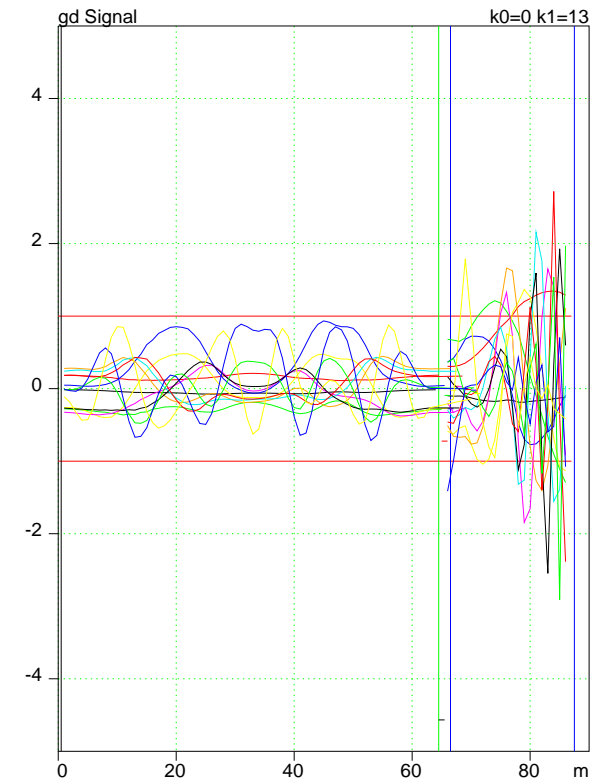
Same case with  $\epsilon_{MSE-LS}^{relative} \rightarrow 0.1\%$  and non-monotonic  $\bar{j}_s$



*q*— profile and variances for all *k*



*p*— profile and its variances as functions of *a*

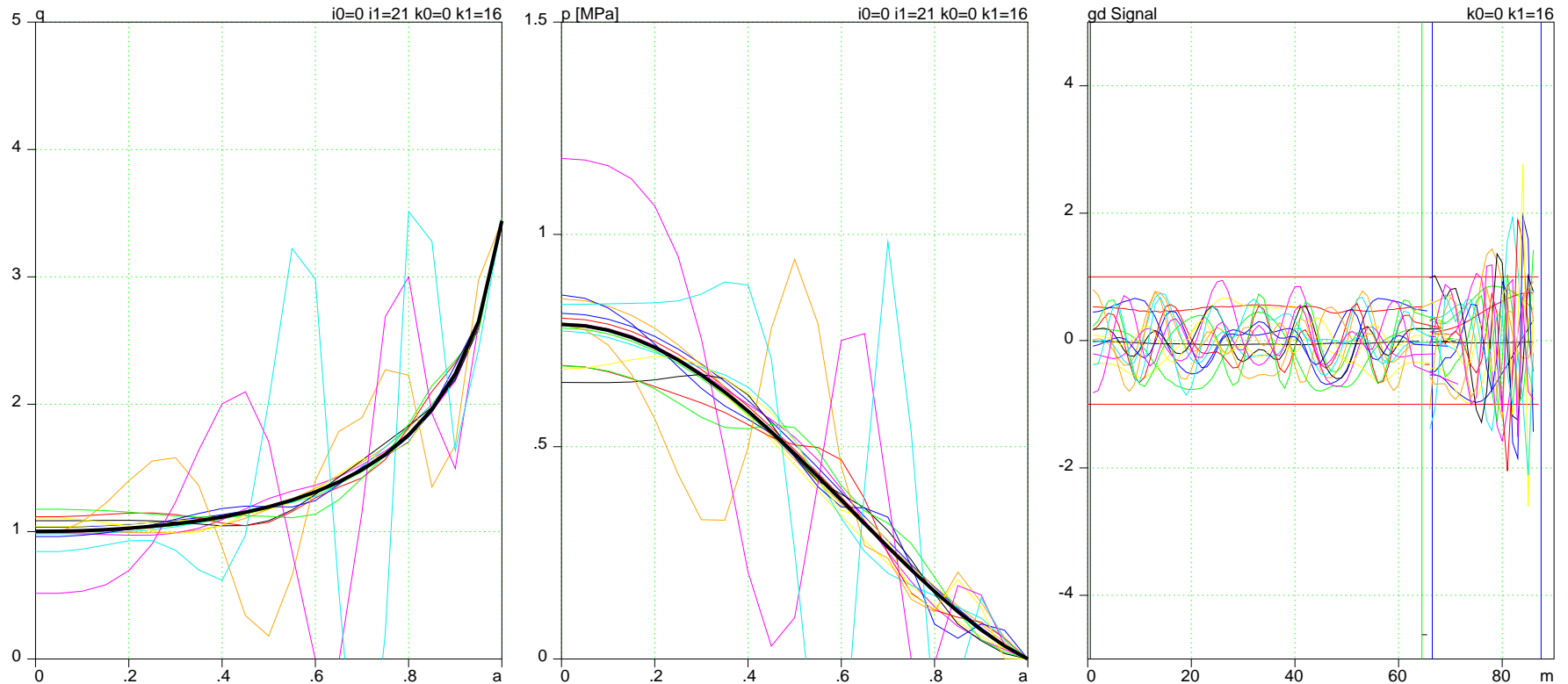


Signals  $\delta S_m / \epsilon_m$  generated by perturbations

**MSE-LS can pick up the details of the current drive**



**Back to reference fixed boundary and ( $\Phi$  &  $B$  & MSE-LS)**



$q$ — profile and variances for all  $k$

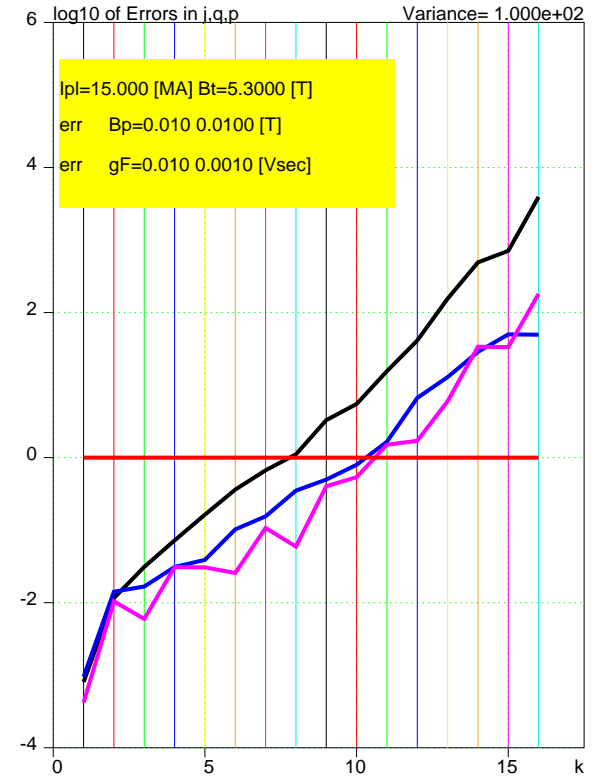
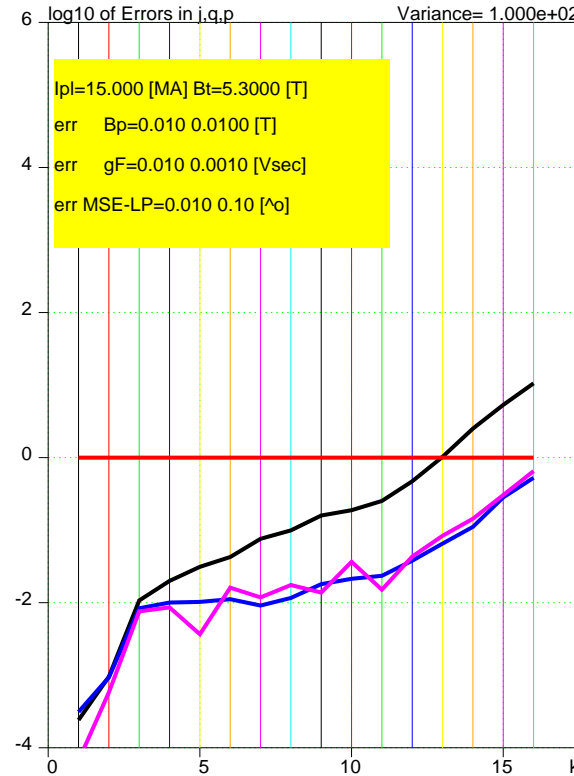
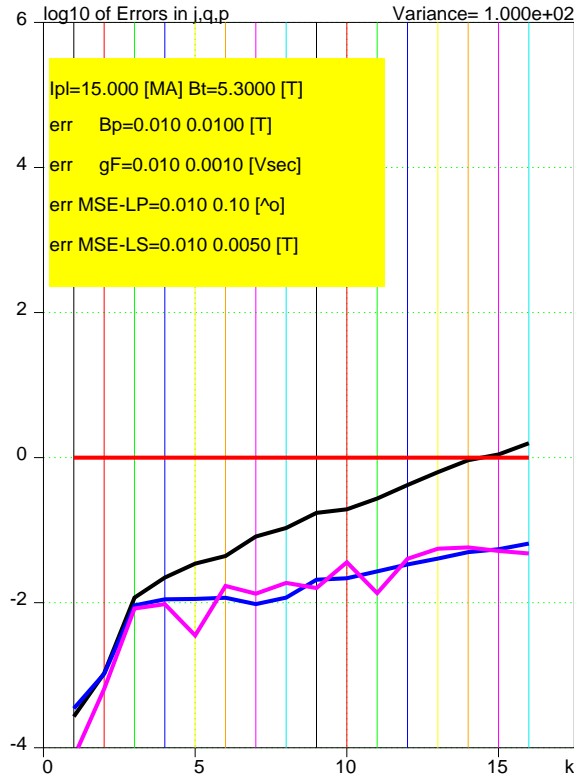
$p$ — profile and its variances as functions of  $a$

Signals  $\delta S_m / \epsilon_m$  generated by perturbations

**With MSE-LS only perturbations with  $k \geq 13$  might be potentially**

**troublesome**

**Fixed plasma boundary with ( $\Phi$  &  $B$  & MSE-LP & -LS) signals**



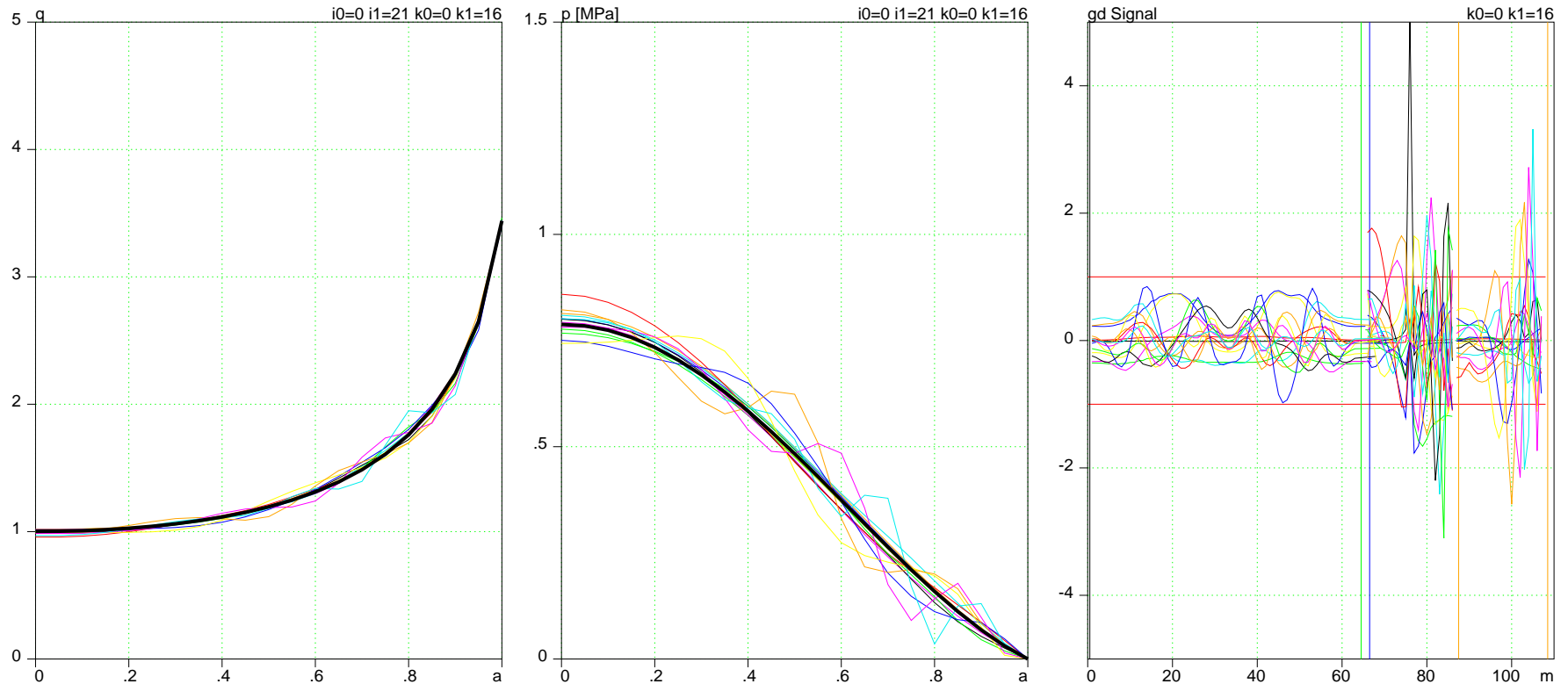
$\log_{10}\{\bar{\sigma}^k, \bar{\sigma}_q^k, \bar{\sigma}_p^k\}$  in case of ( $\Phi$  &  $B$  & MSE-LP & MSE-LS)

$\log_{10}\{\bar{\sigma}^k, \bar{\sigma}_q^k, \bar{\sigma}_p^k\}$  in case of ( $\Phi$  &  $B$  & MSE-LP)

$\log_{10}\{\bar{\sigma}^k, \bar{\sigma}_q^k, \bar{\sigma}_p^k\}$  in case of ( $\Phi$  &  $B$ ) only

**Both MSE-LP & LS allows for a reliable reconstruction of  $q$ - and  $p$ -profiles**

**Fixed plasma boundary with ( $\Phi$  &  $B$  & MSE-LP&LS) signals**



$q$ — profile and variances for all  $k$

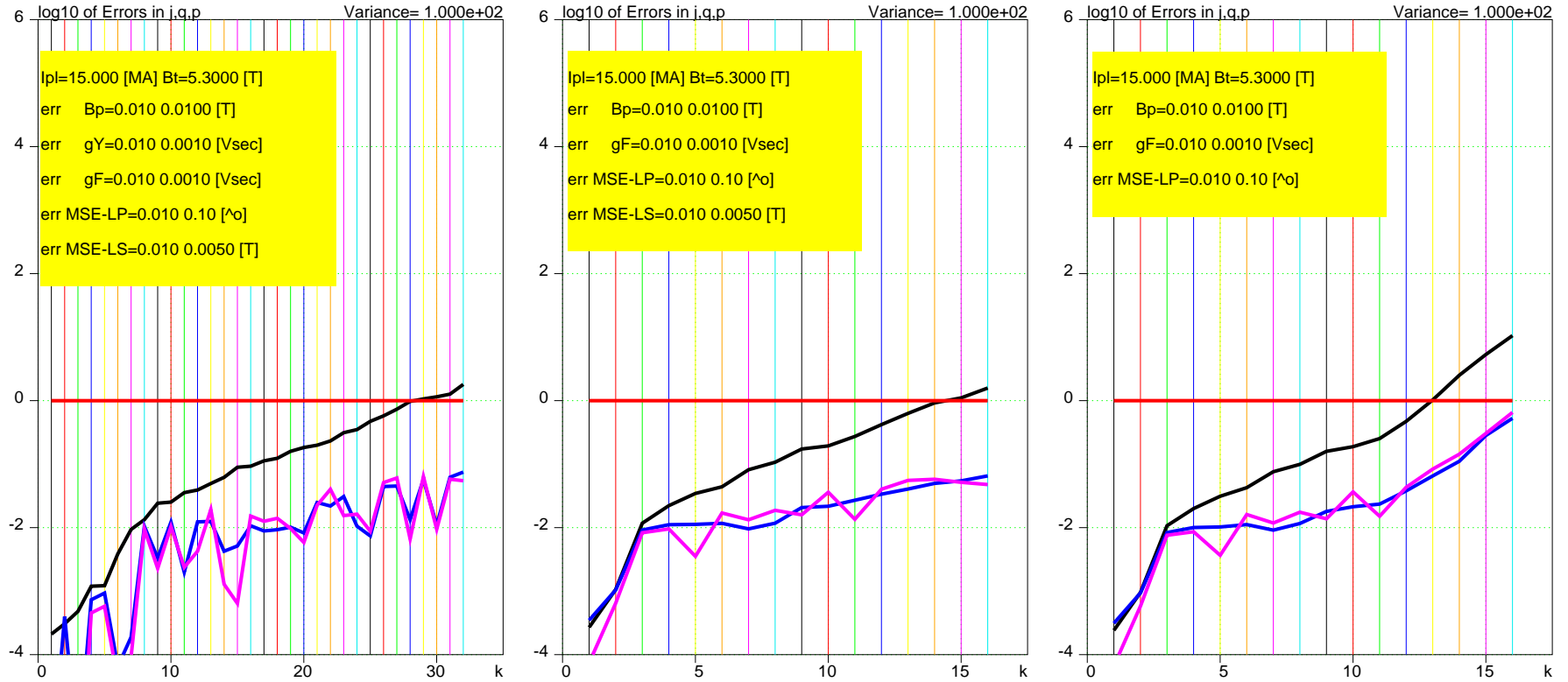
$p$ -profile and its variances as functions of  $a$

Signals  $\delta S_m / \epsilon_m$  generated by perturbations

**$q$ - and  $p$ -profiles can be reconstructed in all spectrum of  $k$**

## 4.5 Free boundary, magnetic signals & both MSE-LP & MSE-LS

### Free boundary plasma with ( $\Phi$ & $B$ & MSE-LP & -LS) signals



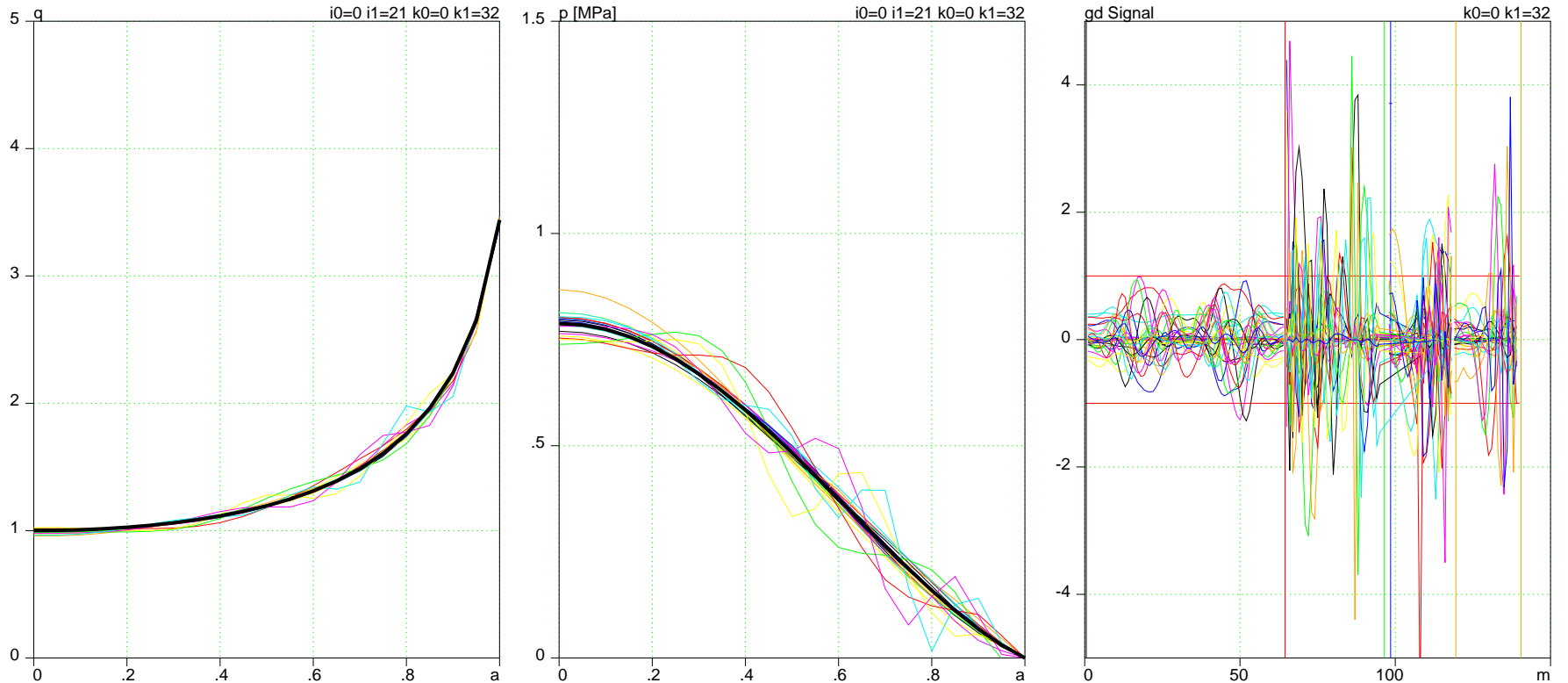
$\log_{10}\{\bar{\sigma}^k, \bar{\sigma}_q^k, \bar{\sigma}_p^k\}$  in case of  
( $\Phi$  &  $B$  & MSE-LP & MSE-LS),  
 $\vec{\xi} \neq 0$

$\log_{10}\{\bar{\sigma}^k, \bar{\sigma}_q^k, \bar{\sigma}_p^k\}$  in case of  
( $\Phi$  &  $B$  & MSE-LP & MSE-LS),  
 $\vec{\xi} = 0$

$\log_{10}\{\bar{\sigma}^k, \bar{\sigma}_q^k, \bar{\sigma}_p^k\}$  in case of  
( $\Phi$  &  $B$  & MSE-LP),  $\vec{\xi} = 0$

**Free boundary expands the  $k$  range but does not affect the reconstruction**

**Free boundary plasma with ( $\Phi$  &  $B$  & MSE-LP & -LS) signals**



$q$ — profile and variances for all extended  $k$

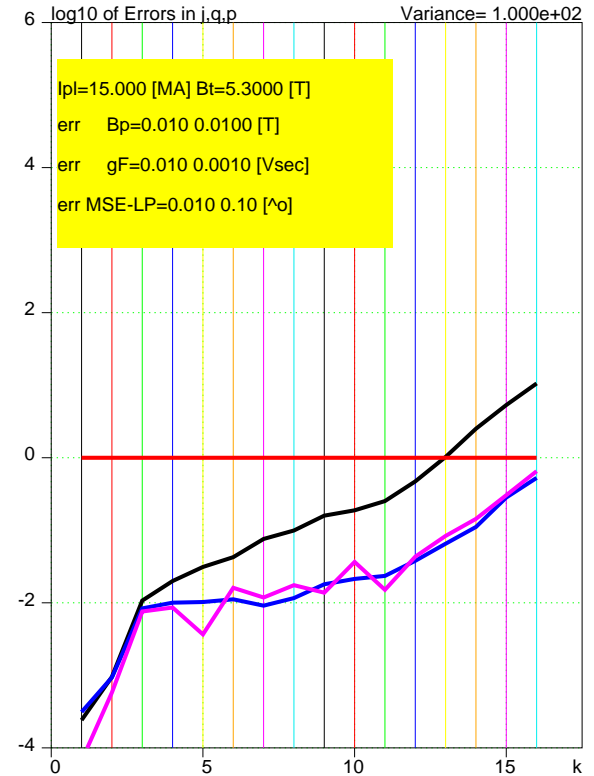
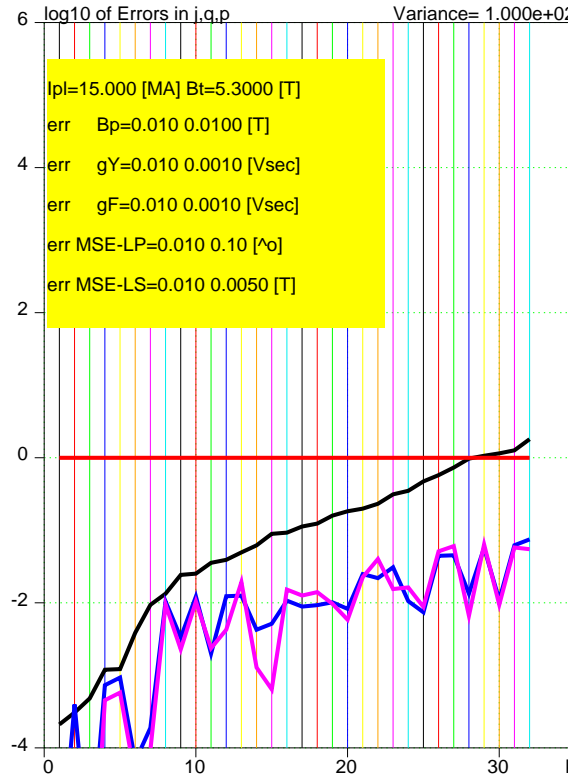
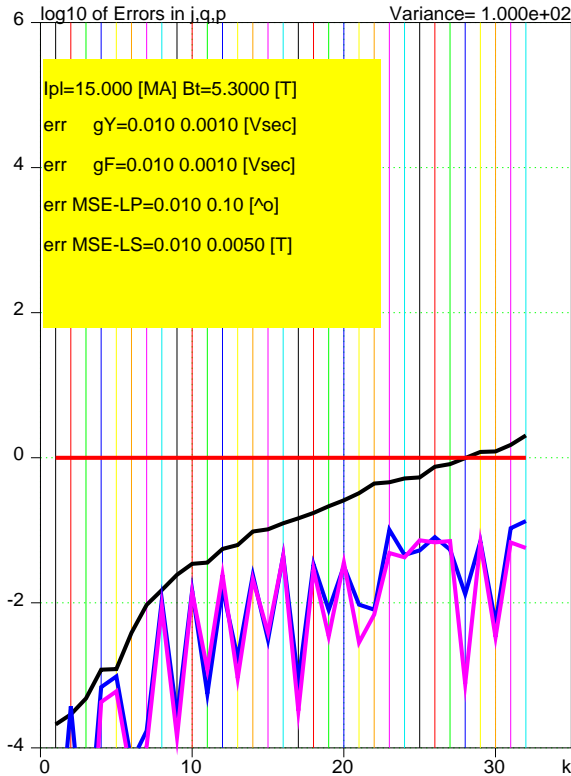
$p$ -profile and its variances as functions of  $a$

Signals  $\delta S_m / \epsilon_m$  generated by perturbations

**$q$ - and  $p$ -profiles can be reconstructed in all extended spectrum of  $k$**

## 4.6 Curious case, NO $B$ -signals, $\xi \neq 0$ , $\Phi$ & both MSE-LP & MSE-LS

### Free boundary, ( $\Phi$ & MSE-LP & -LS) signals, NO $B$ -signals



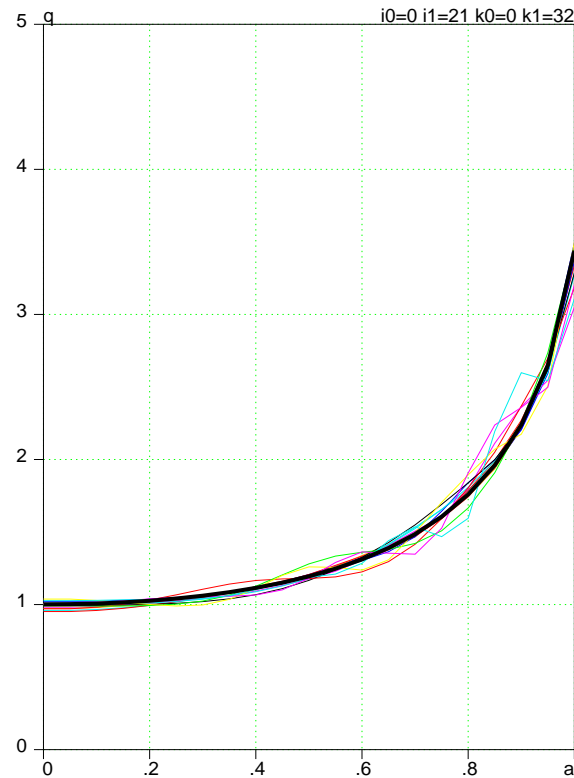
$\log_{10}\{\bar{\sigma}^k, \bar{\sigma}_q^k, \bar{\sigma}_p^k\}$  in case of ( $\Phi$  &  $B$  & MSE-LP & MSE-LS),  $\vec{\xi} \neq 0$

$\log_{10}\{\bar{\sigma}^k, \bar{\sigma}_q^k, \bar{\sigma}_p^k\}$  in case of ( $\Phi$  &  $B$  & MSE-LP & MSE-LS),  $\vec{\xi} \neq 0$

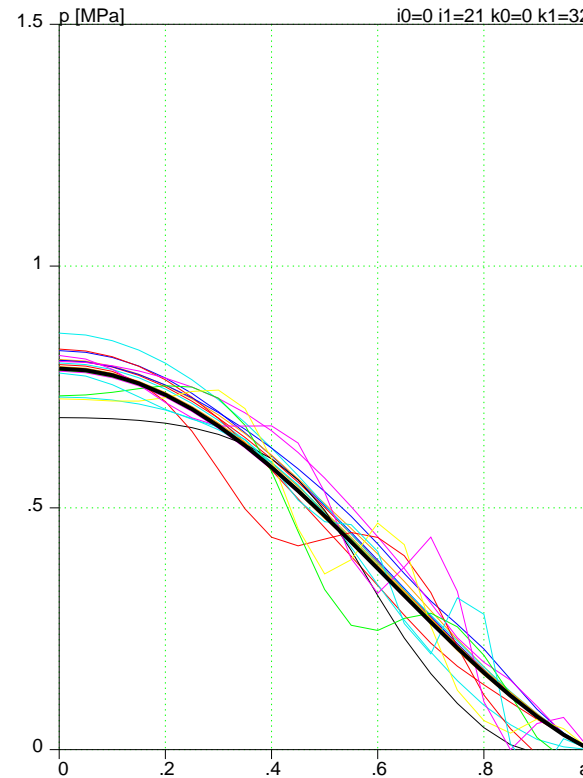
$\log_{10}\{\bar{\sigma}^k, \bar{\sigma}_q^k, \bar{\sigma}_p^k\}$  in case of ( $\Phi$  &  $B$  & MSE-LP), and  $\vec{\xi} = 0$

**(MSE-LP & MSE-LS) together can do the job for external  $B$ -coils**

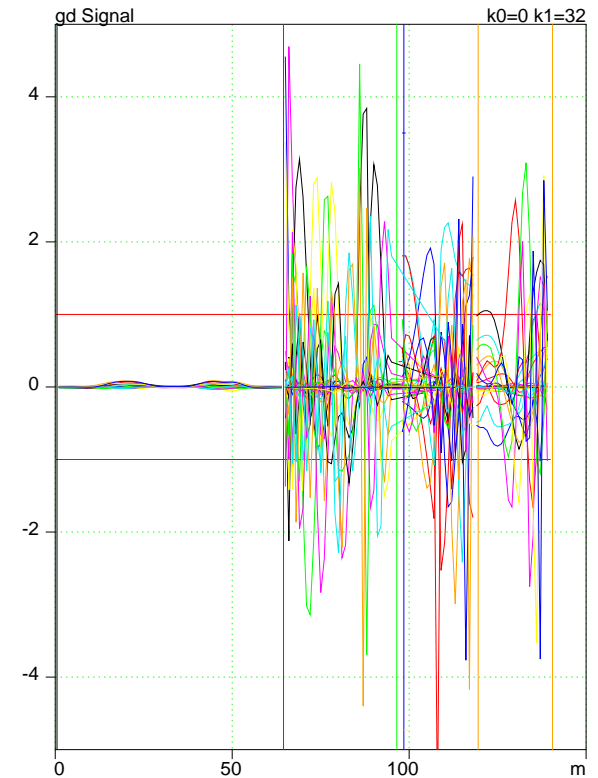
**Free boundary, ( $\Phi$  & MSE-LP & -LS) signals, NO  $B$ -signals**



$q$ — profile and variances for all extended  $k$



$p$ -profile and its variances as functions of  $a$



Signals  $\delta S_m / \epsilon_m$  generated by perturbations

**$q$ - and  $p$ -profiles can be reconstructed over extended spectrum of  $k$**

**even with NO  $B$ -coil signals**

## The capability of calculating variances, now developed, has completed the theory of equilibrium reconstruction

- 1. The quantitative evaluation of the quality of diagnostics systems on existing and future machines can be done based on spectrum of “visible” perturbations*
- 2. It was confirmed that the internal measurements of the magnetic field are crucial for reconstruction.*
- 3. Either MSE-LP (line polarization) or MSE-LS (line shift) signals from the plasma in addition to external measurements allow for a complete reconstruction (of both  $q$ - and  $p$ -profiles).*
- 4. The presented technique can be used to optimize the diagnostic set on any tokamaks. Contribution of any signal can be evaluated.*
- 5. The proposal by Nova Photonics to utilize MSE-LS signals would significantly enhance the equilibrium reconstruction capability in ITER.*

**The extension of the theory should be focused on realistic simulation  
of signals used in reconstructions**